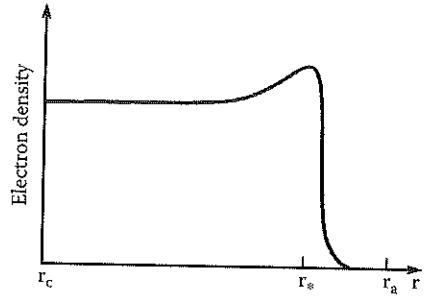

FIGURE 4.23
The variation of the electron density in a layer drifting in crossed electric and magnetic fields. The electrons are emitted from the cathode at r_c, the layer extends outward from the cathode to roughly r_s, and the electrons are insulated by the magnetic field so that they do not cross over to the anode at r_a.

$$(\gamma - 1)mc^2 - e\phi = 0 \tag{4.119}$$

with $\gamma = (1 - v_\theta^2 / c^2)^{-1/2}$. Also, in the absence of azimuthal variations, the canonical momentum in the azimuthal direction is conserved, so that

$$m\gamma v_\theta - \frac{e}{c}A_\theta = 0 \tag{4.120}$$

with A_θ the azimuthal component of the vector potential **A**, which obeys

$$\mathbf{B} = \nabla \times \mathbf{A} \tag{4.121}$$

The magnetic flux is the surface integral of B_z over the cross-sectional area between the cathode and the anode. Because of the high conductivity of the anode and cathode, we assume that the magnetic flux before the voltage is applied, when B_z is the initial applied magnetic field, is the same as the magnetic flux after the voltage is applied, and the diamagnetic effect of the electron layer modifies the magnetic field in the gap. Then the Hull criterion for magnetic insulation of the gap is as follows:

$$B^* = \frac{mc}{ed_e}\left(\gamma^2 - 1\right)^{1/2} = \frac{0.17}{d_e(cm)}\left(\gamma^2 - 1\right)^{1/2} \text{ T} \tag{4.122}$$

measured in Tesla, with

$$\gamma = 1 + \frac{eV_0}{mc^2} = 1 + \frac{V_0(kV)}{0.511} \tag{4.123}$$

with V_0 the anode–cathode voltage and d_e the effective gap in cylindrical geometry,

$$d_e = \frac{r_a^2 - r_c^2}{2r_a} \tag{4.124}$$

When $B_z > B^*$, the critical magnetic field or Hull field, the electrons drift azimuthally within a bounded electron cloud called the Brillouin layer. As $B_z \to B^*$, the electron cloud extends almost to the anode. As the magnetic field increases, the cloud is confined closer and closer to the cathode. Remarkably, even though Equation 4.122 takes account of collective space-charge and diamagnetic effects from the electron layer, it is exactly the result one would obtain if one set the Larmor radius for a single electron equal to d_e (see Problem 16).

4.8 Microwave-Generating Interactions

We can understand the microwave generation process in HPM sources in terms of resonant interactions between the normal modes of a cavity or waveguide and the natural modes of oscillation in a beam or electron layer. To impose some order on the discussion of microwave sources, we classify them according to various criteria. From the standpoint of the electromagnetic normal modes, sources are said to be either *fast-wave* or *slow-wave* devices. A fast-wave interaction involves a waveguide mode with a phase velocity that is greater than the speed of light, as in the smooth-walled waveguides of Section 4.3, while a slow-wave interaction involves a mode with a phase velocity less than the speed of light, as in the slow-wave structures of Section 4.4.

From the standpoint of the electrons participating in the generation process, we define three classes of devices:

- *O-type*: Devices in which the electrons drift parallel to an externally imposed magnetic field. This field helps to guide the intense beams used in HPM sources and, in some instances, plays an essential role in the microwave generation process.
- *M-type*: Devices in which the electrons drift perpendicularly to crossed electric and magnetic fields.
- *Space-charge*: Devices, possibly involving an applied magnetic field, in which the interaction producing microwaves is intrinsically traceable to an intense space-charge interaction.

The interactions leading to microwave generation in both the O- and M-type devices produce waves that grow up from small perturbations on an initial equilibrium state. The situation is quite different in the space-charge devices. The flow of the electrons in those devices is disturbed in a way that prevents the existence of an equilibrium; however, the resulting oscillatory state has a natural frequency. Thus, there are similarities in the operation of the O- and M-type sources that are not shared with the space-charge devices. We will briefly review the common elements of the first two types of sources before considering each source type individually.

4.8.1 Review of Fundamental Interactions

In O- and M-type devices, microwaves are generated primarily by linear resonances in which the waveguide or cavity normal modes and the electron oscillations must have the same frequency. Further, they both must have the same phase velocity, ω/k_z, so that they advance together along the system axis. Therefore, the values of ω and k_z for the two waves must be equal. In many cases, the properties of each of the electromagnetic and electron waves are largely independent of one another, except at values of ω and k_z in the vicinity of the resonance. Hence, we can estimate the resonance frequency and wavenumber by looking for the intersection in an ω-k_z plot of the dispersion curves for an electromagnetic normal mode (examples of which are shown in Figure 4.4, Figure 4.9, and Figure 4.15) and one of the oscillatory modes of the electrons. However, not all such interactions are truly resonant, permitting the transfer of electron energy to microwaves. The issue of which intersections lead to resonant microwave generation is resolved by deriving and solving the full dispersion relation for a coupled system of electromagnetic waves and electrons. In such a calculation, near microwave-generating resonances ω and k_z are in general complex, with the result that an *instability* exists and the waves exhibit exponential spatial and temporal growth.

More in line with our approach of treating the electromagnetic and particle modes as almost independent, the incremental wave energy of the participating modes, calculable from uncoupled dispersion relations, can be considered to determine if an interaction will be unstable.[16,17] When an intersection in the dispersion diagrams leads to microwave generation, the electron oscillation participating in the resonance is said to be a *negative energy wave* in the following sense. The total energy of the coupled system, including the electromagnetic energy of the normal mode and the summed energy of the electrons, is positive; however, the total energy is higher in the initial equilibrium state with no electron oscillations than it is in the presence of the unstable electron oscillation. The electron oscillation therefore reduces the total energy of the system and has a negative energy in the incremental sense. This energy reduction does not occur for some electron oscillations, which are said to be *positive energy waves*; these will not interact unstably with the electromagnetic normal modes, which always have a positive energy, and they cannot be used to generate microwaves. We will shortly return to this point in the specific case of space-charge waves.

In most sources, wave growth is accompanied by *bunching* of the electrons in one way or another. For example, in some devices, the electrons form spatial bunches, while in others, they bunch in the phase of their rotation about the magnetic field lines. In any event, bunching is an important phenomenon because it enforces the coherence of the electromagnetic waves that are generated.[18] To understand this, think of the generation process as an emission process by the individual electrons. In a uniform beam of electrons, the phases of the waves emitted by the individual electrons are completely random, so that the sum total of the radiation emitted by all of the electrons cancels out. Due to the action of the waves back onto the beam, however, the beam forms into bunches, the phases of the waves from each electron are no longer random, and the net sum of the emitted waves becomes nonzero. Thus, bunching makes the difference between the incoherent spontaneous emission of the initial state and the coherent stimulated emission of the later state. When the beam is strongly bunched,[19] the microwave output power is proportional to the number of bunches, N_b, and the square of the number density of electrons within the bunches, n_b:

$$P \propto N_b n_b^2 \tag{4.125}$$

Of course, the process of wave growth and bunching cannot proceed indefinitely; eventually, if given enough time, the instability will proceed to *saturation* and wave growth ceases, as shown in Figure 4.24. A variety of mechanisms lead to saturation, but two are seen most commonly: either the excess kinetic energy of the electrons is exhausted and the electron oscillation falls out of resonance, or the electron bunches become trapped in the strong potential wells of the electromagnetic waves and begin to reabsorb energy from the wave as they "slosh" around the well.

4.8.2 O-Type Source Interactions

At root, there are only a couple of basic interactions underlying the operation of the O-type devices. One is based on the oscillation of *space-charge waves* on an electron beam. To understand these, imagine a very long, large-diameter beam of electrons drifting along the z axis of a metallic drift tube, confined in the radial direction by a very strong axial magnetic field. If the density of the beam is uniform, axial forces along the beam are negligible, except near the ends. Imagine, though, that the electrons are squeezed together in one area, creating an electron bunch. The effect is like that of squeezing a section of spring together; the space-charge forces between the electrons in the bunch will cause them to repel one another and move apart, overshooting to create higher-density bunches on either side of the original

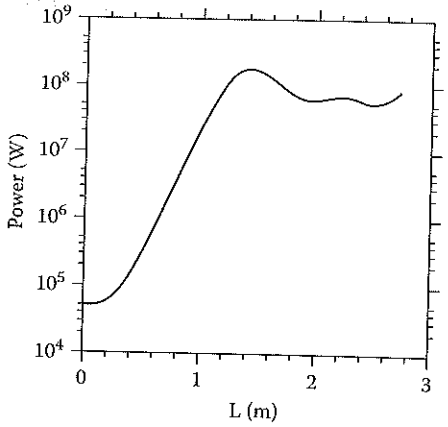

FIGURE 4.24
The growth to saturation of a microwave signal as a function of distance along the interaction region, L.

bunch, which once again repel one another and so move back together, creating an oscillation back and forth. The relation between the oscillation frequency and the axial wavenumber of the oscillations is

$$\omega = k_z v_z \pm \frac{\omega_b}{\gamma_0} \tag{4.126}$$

where $\omega_b = (n_b e^2 / \varepsilon_0 m \gamma_b)^{1/2}$ is the *beam plasma frequency* for a beam of electron number density n_b and electron velocity v_z, with $\gamma_b = (1 - v_z^2 / c^2)^{-1/2}$ the relativistic factor. The waves with the two frequencies in Equation 4.126 are commonly known as the fast and slow space-charge waves, according to the use of the + or – sign, respectively.

The importance of boundary conditions was stressed in Section 4.2, yet Equation 4.126 contains no geometrical factors and is derived quite simply without regard for the radial boundaries of a real configuration. Analysis shows, though, that the dispersion relation for space-charge waves on a bounded beam in a waveguide is modified in some significant ways when the boundary conditions are taken into account. Figure 4.25 shows the dispersion relation for the space-charge waves in a beam within a waveguide (derived by Brejzman and Ryutov[20]), compared to the infinite cross-section model appropriate to Equation 4.126. The primary difference occurs near $k_z = 0$, where Equation 4.126 gives a wave with a phase velocity greater than the speed of light, whereas the solution to the actual dispersion relation shows that the phase velocity of the space-charge waves is always less than c (note that even the "fast" space-charge wave is a slow wave in this sense). In either case, with or without radial boundary conditions taken into account, the slow space-charge wave is the negative energy wave, while the fast space-

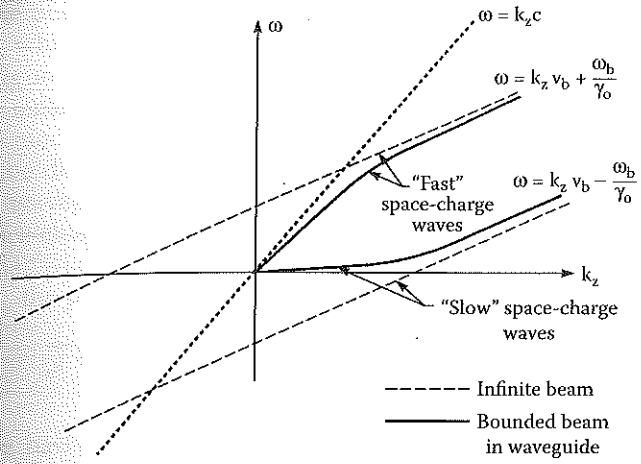

FIGURE 4.25
The space-charge wave dispersion diagram for an unbounded beam model (dashed) and a beam in a waveguide (solid).

charge wave has a positive incremental energy. Microwave generation occurs at a frequency and wavenumber approximately given by the intersection between the dispersion curves for the slow space-charge wave and an electromagnetic normal mode; intersections between curves for the fast space-charge wave curve and a normal mode will not yield a microwave-generating resonance.

The slow space-charge waves, with $\omega/k_z < c$, cannot couple to the normal modes of a smooth-walled waveguide, which have $|\omega/k_z| > c$. Nevertheless, there are ways to achieve the required coupling between the space-charge wave and an electromagnetic normal mode. For example, the phase velocity of the waveguide modes can be reduced below the vacuum speed of light by inserting into the guide a dielectric material with a permittivity, ε, significantly greater than that of vacuum, ε_0 (for example, a rod on axis, a sleeve inside the walls, or even a plasma layer), so that the effective speed of light in the waveguide appearing in Equations 4.20 and 4.21 approaches $c' = c(\varepsilon_0 / \varepsilon)^{1/2}$. When c' is made less than v_z, as shown in Figure 4.26a, the resulting resonance between the slow space-charge wave and the electromagnetic mode serves as the basis of the *dielectric Cerenkov maser* (DCM).[21]

The guide modes can also be slowed down by modifying the shape of the walls of the guide to create a *slow-wave structure*, such as those we discussed in Section 4.4. The periodic slow-wave structures of Section 4.4 are the bases of devices like the *backward wave oscillator* (BWO) and *traveling wave tube* (TWT) described in Chapter 8, when the variation in slow-wave-structure radius is along the axis. Distinguishing between the BWO and TWT requires a knowledge of the dispersion curves and the location of the intersection between the slow space-charge wave and the slow-wave-structure curve: BWOs result when the slow-wave-structure dispersion curve has a negative

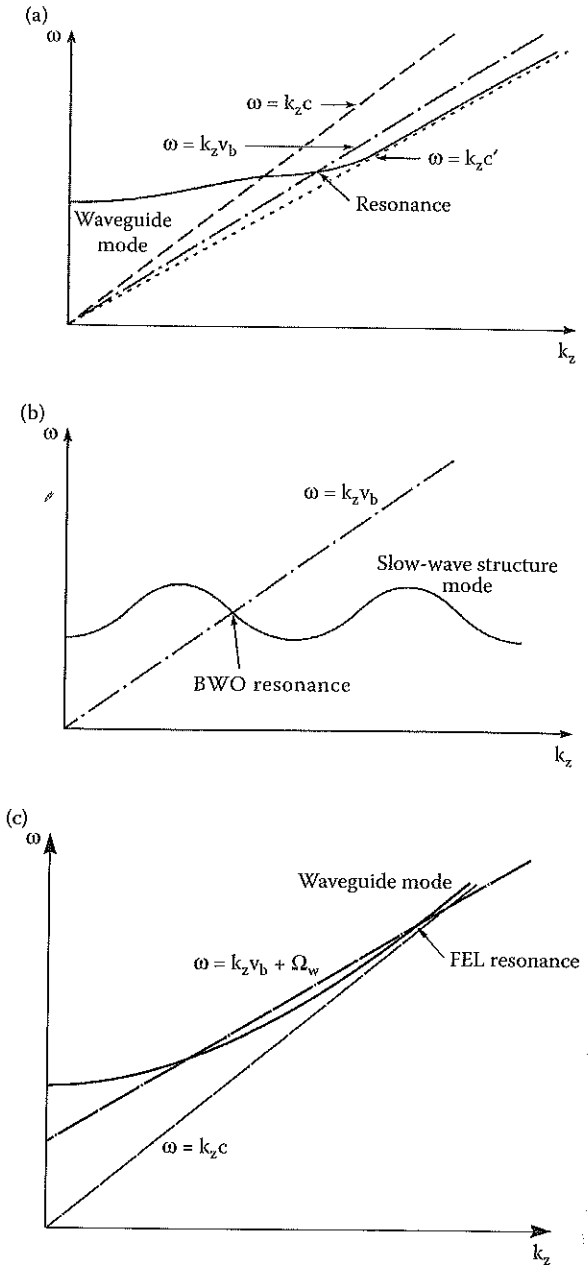

FIGURE 4.26
Uncoupled dispersion relations for systems in which the space-charge waves interact with differing electromagnetic modes: (a) dielectric Cerenkov maser, (b) backward wave oscillator, and (c) free-electron laser.

slope at the point of intersection, so that the group velocity is negative, or backward, while TWTs involve an intersection at a point of positive group velocity. Figure 4.26b illustrates such a resonance for a BWO.

A third means of coupling slow space-charge waves to guide modes involves a modification not of the waveguide dispersion, but of the space-charge wave dispersion. If a periodic transverse magnetic field is applied inside the waveguide, one view of the result is that the dispersion curves for the space-charge waves have been upshifted in frequency by an amount equal to the "wiggle" frequency of the electrons, $\omega_w \approx k_w v_z$, where $k_w = 2\pi/\lambda_w$ with λ_w the periodicity of the magnetic field, so that

$$\omega \approx k_z v_z + \omega_w \tag{4.127}$$

This is the basis for the *free-electron laser* (FEL), or *ubitron*, described in Chapter 10. Hence, in this view of FEL operation, the space-charge waves are made into fast waves capable of interacting with the fast waveguide modes. Alternatively, the radiation process can be viewed as magnetic bremsstrahlung, or coherent synchrotron radiation of the transversely accelerated electrons. Figure 4.26c depicts this resonance. Note that there are two intersections between the upshifted slow space-charge mode and the waveguide dispersion curve. Characteristically, FEL operation is at the upper intersection (see Problem 16).

The *relativistic klystron*, discussed in Chapter 9, makes use of resonant cavities to excite the space-charge waves on the beam. The simplest two-cavity form of the klystron is shown in Figure 4.27. The beam interacts with a normal mode of the first cavity (which is usually driven externally), and the fields associated with this electromagnetic mode modulate the axial drift velocities of the beam electrons and excite space-charge wave growth on the beam. In the drift space between the two cavities, the space-charge wave growth continues. The resulting space-charge bunches then pass into the second cavity, where they excite an electromagnetic cavity mode, the fields of which can be coupled out as radiation. A distinguishing feature of the klystron is that the only communication between the two cavities is through

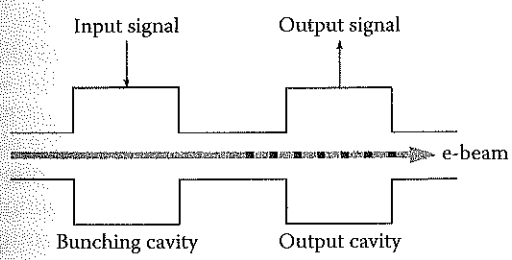

FIGURE 4.27
The simplest two-cavity form of a klystron.

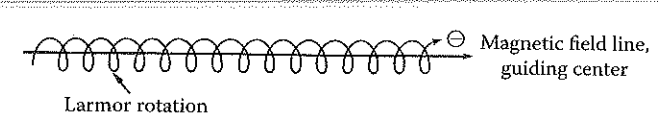

FIGURE 4.28
Larmor rotation at the electron cyclotron frequency, ω_c, about the guiding center, which lies along a magnetic field line.

the space-charge waves, since the drift space between the cavities is made sufficiently small that it is cut off to the propagation of the cavity modes between the two (recall that the cutoff frequency $\omega_{co} \propto 1/r_0$). In fact, this requirement becomes quite restrictive as the desired operating frequency increases, since cutting off the lowest frequency waveguide mode, TE_{11}, means that for an operating frequency f, the waveguide radius must be less than a maximum value of $r_{max}(cm) = 8.8/f(GHz)$. One way of getting around this is to cut off all but the few lowest frequency modes, and then design the drift tube between cavities in such a way that the lowest-order modes cannot propagate (e.g., by cutting properly shaped slots in the walls or loading them with a microwave absorber).

An entirely different mechanism for generating microwaves from a magnetized beam of electrons involves electron–cyclotron interactions with the beam electrons. Consider a beam traveling along a reasonably strong guide field, but imagine that the individual electrons have a velocity component perpendicular to $\mathbf{B}_0$, so that they execute small-orbit Larmor rotation about their guiding centers at the cyclotron frequency $\omega_c = eB_0/m\gamma_b$, as shown in Figure 4.28. The individual electrons can then spontaneously emit Doppler-shifted cyclotron radiation of frequency

$$\omega = k_z v_z + s\omega_c \tag{4.128}$$

with s an integer. Electrons emitting this radiation can interact resonantly with the fast waveguide modes, and because the cyclotron frequency is energy dependent (as $1/\gamma_b$), the rotating electrons will become bunched in their rotational phase (which is entirely different from the spatial bunching of the space-charge waves). This resonance is the basis for a number of *electron cyclotron maser* types, such as the *gyrotron* and *cyclotron autoresonant maser* (CARM), described in Chapter 10 (see Problem 4).

Our interpretation of the microwave-generating resonance in the devices considered so far — the BWO and TWT, the FEL, and the electron cyclotron masers — has been constructed in terms of interacting collective modes. We can alternatively view the radiation process as the action of a coherent ensemble of transversely accelerated electrons that are emitting. In the FEL, where electrons undulate in the wiggler field, and the gyrotron, where the electrons gyrate about field lines, this phenomenon is readily apparent. On the other hand, in the BWO and TWT, the physical picture is modified somewhat. In those devices, the charge density perturbations in the space-charge waves on the beam create image charges in the rippled-wall slow-wave structure, and it is these image charges, moving transversely with the wall ripple, that can be viewed as causing a kind of dipole radiation as they convect along with the beam space-charge waves.

An additional interaction of some interest is that in which two types of beam modes work together parametrically to produce a third wave, an electromagnetic output. To take an example, if a slow space-charge wave becomes large enough in amplitude, it can function as the wiggler to drive an FEL-type interaction, even in the absence of a magneto-static wiggler field. This type of stimulated scattering[22] has been used in two-stage FELs, for example, in which the first stage is either another FEL[23] or a BWO.[24] Such devices are sometimes called *scattrons* in the Soviet and Russian literature.

As a final point in the discussion of O-type devices, we note that the klystron concept — setting some form of bunching in motion in one interaction region, propagating the beam through a cutoff waveguide section, and then tapping the bunched beam in a separated, downstream interaction region — has quite general applicability and has been employed in the design of several hybrid devices. For example, the *gyroklystron* essentially features gyrotron resonators separated by waveguides in which gyrophase bunching occurs (see Chapter 10). A second example is the *optical klystron* (Chapter 10), which is a variant of the FEL with multiple interaction spaces. In devices of this type, the advantage of the klystron principle is that it makes a pre-bunched beam available to the downstream cavity (or cavities, if the bunching process is enhanced by using more than a single cavity), where the bunching enhances the efficiency.

4.8.3 M-Type Source Interactions

In contrast with O-type devices, electrons in M-type devices drift across a magnetic field in crossed electric and magnetic fields. This type of motion is called an $\mathbf{E} \times \mathbf{B}$ drift. Most commonly, M-type devices involve the interaction between a slow-wave electron mode and electromagnetic normal modes directed colinearly with the overall drift of the electrons. The primary example of such a device is the *relativistic magnetron*, depicted schematically in Figure 4.29 and discussed in Chapter 7. There, an electron layer drifts azimuthally near the cathode of a cylindrical diode in the radial electric field and applied axial magnetic field. Because the cavity is closed on itself in the azimuthal direction (or reentrant, in the accepted parlance), counterrotating electromagnetic modes can set up a standing wave pattern around the cavity. It has become the convention in the case of magnetrons to characterize the normal cavity modes by the phase shift of the waves between the individual resonators. Electromagnetic modes with phase shifts of π and 2π, known as the π-mode and 2π-mode, are the most commonly seen operating modes in magnetrons. In addition to the magnetron, an amplifying M-type source

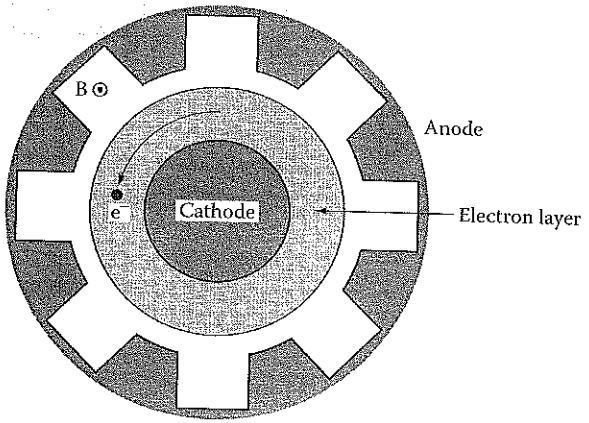

FIGURE 4.29
Schematic depiction of a magnetron cavity, in cross section.

known as the *crossed-field amplifier* has existed in the nonrelativistic regime for some time, and one was briefly explored in the high power regime. More recently, a linear device with high power potential known as a *magnetically insulated line oscillator* (MILO) has been explored.

A fast-wave M-type device has also been examined. In this device, known as a rippled-field magnetron, the slow-wave structure of Figure 4.29 is replaced with a smooth wall into which permanent magnets of alternating polarity have been placed. Thus, the device is like a cylindrical FEL in which the beam has been replaced by a magnetically insulated layer of electrons undergoing $\mathbf{E} \times \mathbf{B}$ drifts.

4.8.4 Space-Charge Devices

Space-charge devices are so named because their operation depends on a strong space-charge-driven phenomenon involving the formation of a virtual cathode. The best-known device of this type is the *virtual cathode oscillator*, or *vircator*. To understand its operation, consider the configuration shown in Figure 4.30. There, an electron beam is generated in a diode with a thin-foil anode that allows the beam to pass through to the drift space beyond. For a cylindrical drift space, the situation is that discussed in Section 4.6.3. If the drift space has grounded walls and a radius r_0, while the beam has radius r_b and was launched from a cathode at voltage $-V_0 < 0$, the space-charge-limited current I_{SCL} for the drift space is given by Equation 4.115 if the beam cross section is annular and Equation 4.116 if the beam cross section is solid. A beam current I_b exceeding the appropriate value of I_{SCL} will cause the formation of a strong potential barrier at the head of the beam, from which a significant number of the beam electrons will be reflected back toward the anode. The reflection point for the electrons is

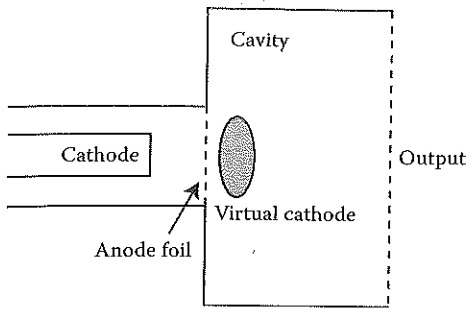

FIGURE 4.30
Schematic depiction of a virtual cathode oscillator, or vircator.

known as the virtual cathode. Essentially, the excess space-charge in the beam is rejected from the drift space. This situation is intrinsically different from the other microwave generation mechanisms we have discussed to this point, because in the earlier cases, we started with a well-defined initial beam state on which perturbations grew up from small amplitudes at early times. In the case of virtual cathode formation, there is a very fundamental breakdown of the beam state with the result that no beam equilibrium is possible. The position of the virtual cathode oscillates axially, shedding charge and behaving like a relaxation oscillator. The motion of the space-charge and potential well of the virtual cathode produces radiation at a frequency that is proportional to the square root of the beam current (for solid beams, it is of the order of the beam plasma frequency, ω_b). The bandwidth of the vircator is quite large, and if the virtual cathode is formed in a resonant cavity, it will interact with the cavity modes to oscillate at a frequency tuned to a cavity mode.

The second type of space-charge device, the *reflex triode*, is configured somewhat similarly to the vircator, as shown in Figure 4.31, except that

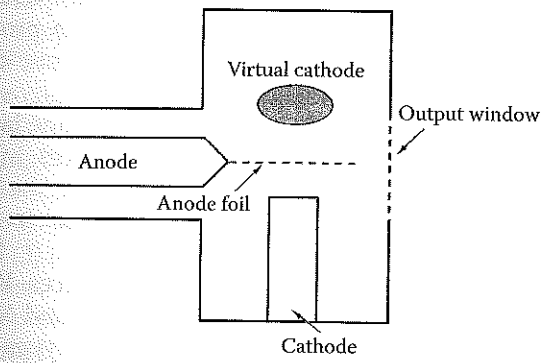

FIGURE 4.31
Schematic depiction of a reflex triode.

TABLE 4.5

Classification of HPM Sources

	Slow Wave	Fast Wave
O-Type	Backward wave oscillator	Free-electron laser (ubitron)
	Traveling wave tube	Optical klystron
	Surface wave oscillator	Gyrotron
	Relativistic diffraction generator	Gyro-BWO
	Orotron	Gyro-TWT
	Flimatron	Cyclotron autoresonance maser
	Multiwave Cerenkov generator	Gyroklystron
	Dielectric Cerenkov maser	
	Plasma Cerenkov maser	
	Relativistic klystron	
M-Type	Relativistic magnetron	Rippled-field magnetron
	Cross-field amplifier	
	Magnetically insulated line oscillator	
Space-Charge	Vircator	
	Reflex triode	

the anode, rather than the cathode, is attached to the center conductor of the transmission line feeding power to the source. If the anode were perfectly transmitting with no absorption of electron energy, an electron from the cathode would drop down to the potential well at the anode, then roll up the other side of the well to the virtual cathode to be reflected back toward the cathode, where it would come to rest after passing back through the anode. Actually, though, some electron energy will be lost in the anode, and electrons will almost, but not quite, reach the emitting cathode, after which they will pass back through the anode, losing a little more energy on each pass, falling short of the original cathode, turning back toward the anode again, and on and on until all of the electron energy is lost. This reflexing back and forth by the electrons provides another source of microwaves for a device known as the reflex triode. A point to note is that in the simple vircator of Figure 4.30, both processes, virtual cathode oscillations and reflexing, can compete with one another unless special care is taken.

As we shall see in Chapter 9, the operation of low-impedance relativistic klystrons has some similarity to the space-charge devices, in that when the beam current exceeds a time-dependent limiting value in the klystron cavity gaps, current bunching takes place almost immediately in the vicinity of the gap.

Table 4.5 summarizes our classification of HPM sources. We can see that there are fast- and slow-wave devices for both the O- and M-type sources. We do not distinguish between fast- and slow-wave types for the space-charge devices. Some source varieties not shown in the table can be found in the later sections of this book, but these represent, in many cases, variations on the basic types discussed here.

4.9 Amplifiers and Oscillators, High- and Low-Current Operating Regimes

The classification system in Table 4.5 is based on the nature of the microwave-generating interactions. We could choose an operational criterion for grouping our sources, however. Let us therefore distinguish between *amplifiers* and *oscillators*. An amplifier produces an output signal that is a larger amplitude version of some input signal; in the absence of an input signal, there is usually no output signal other than low-level amplified noise. An oscillator, on the other hand, requires (1) feedback and (2) sufficient gain to overcome the net losses per cycle, so that an output signal can be generated spontaneously even in the absence of an input signal. Since gain typically increases with beam current, the requirement for sufficient gain is usually translated into a threshold condition on the beam current, called the *start current* for oscillations. Below this value, the system will not oscillate spontaneously, while above it, spontaneous signals will result. The start current is a function of system parameters, including the length of the interaction region.

Amplifiers are characterized by a certain finite bandwidth of input signal frequencies over which useful amplification is possible, while oscillators tend to select a very definite frequency of operation, depending again on the resonant frequency between the beam and the cavity. The output characteristics of an amplifier — frequency, phase, and waveform — can be controlled quite nicely with the provision of a low power master oscillator with the desired features. Designing for high gain and output power while controlling the tendency to break into spontaneous oscillation can be difficult, though. Features of oscillators that are frequently important for applications are *frequency pushing*, the variation of the frequency with source current; *frequency pulling*, the variation of frequency with change of phase of the complex impedance of some load connected to the oscillator cavity; and *phase jitter*, the pulse-to-pulse variation of the initial phase of oscillations. Oscillators enjoy the simplicity attendant to the absence of a master oscillator, although phase and frequency control, to which we will return in the next section, is more complicated than for an amplifier.

Some sources are suited to operation exclusively or primarily as either oscillators or amplifiers. Those usually operated as oscillators are (1) BWOs, because of the feedback inherent in the coupling to a backward wave normal mode; (2) gyrotrons, due to the low-group-velocity, high-Q cavity mode employed; and (3) magnetrons and rippled-field magnetrons, since they use reentrant cavities. Nevertheless, BWOs and gyrotrons can, in principle, function as amplifiers below their start currents. As their name implies, crossed-field amplifiers are designed to be amplifiers by the inclusion of a short absorbing section meant to prevent the complete, 2π circulation of electromagnetic waves around the source azimuth. The other sources of Table 4.5 — cyclotron autoresonance masers (CARMs), FELs, MILOs, TWTs,

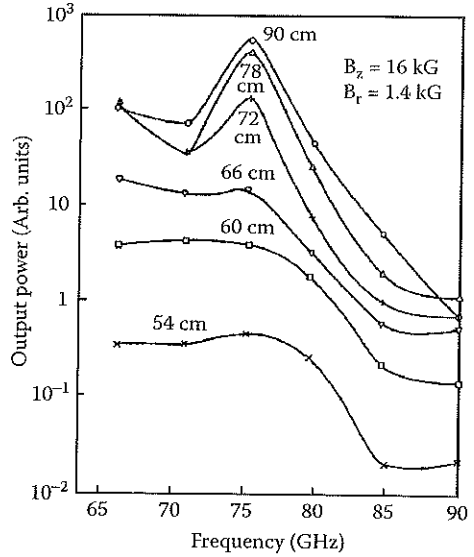

FIGURE 4.32
The output of a super-radiant FEL amplifier. Measurements were made at the frequencies indicated, and points taken for devices of the same length were connected to make the curves shown. (From Gold, S.H. et al., *Phys. Fluids*, 27, 746, 1984. With permission.)

and Cerenkov masers — all have open configurations and forward-directed normal modes, so they all operate primarily as amplifiers. Additionally, they can be run as oscillators if some type of feedback is introduced, such as reflections at the downstream end.

Midway between amplifiers and oscillators, there are the *super-radiant amplifiers*. Although they are not, strictly speaking, a separate device type, these are amplifiers with such a high gain that they will amplify spontaneous noise on the beam to high output power levels. In a sense, the effect is like that of an oscillator, with the difference that the line width of the output (i.e., the spectral width of the output frequency) is broader. Lengthening such a device can narrow the line width about the frequency of the mode with the highest gain. An example of the output from a super-radiant FEL amplifier is shown in Figure 4.32. There, we see the noticeable peaking of output as a function of frequency as the device is lengthened.

A third, very broad means of classifying microwave sources is according to the intensity of the space-charge effects in the device. At low electron densities, typically corresponding to low beam currents, a device is said to be in the *Compton* regime of operation. In this case, collective space-charge effects are negligible and the electrons behave as a coherent ensemble of individual emitters. At high electron densities, with beam currents approaching a significant fraction of the space-charge limit, the collective modes of electron oscillation (e.g., space-charge waves) play the central role in microwave generation. This is called the *Raman* regime of operation. Some authors might distinguish intermediate states between these two extremes, but this simple delineation will serve our purposes.

4.10 Phase and Frequency Control

Phase and frequency control of a microwave signal are desirable in a variety of applications, such as driving radio frequency accelerators, maximizing the spatial power density from a multiple-antenna array, and even electronically steering the output of such an array. As we mentioned in the previous section, perhaps the most straightforward means of controlling the phase of an array of sources is to generate the high power from one or more power amplifiers driven by a relatively lower power master oscillator. This configuration is denoted by the acronym MOPA (master oscillator/power amplifier). The difficulties inherent in the design of high power, high-gain amplifiers and the complexity of MOPA arrays leave room for the use of phase- or frequency-controlled oscillators.

Phase locking and frequency control of oscillators can be achieved in several ways. Perhaps the most common involves the use of the power from a driving master oscillator to determine the phase of a slave oscillator. The important parameter is the injection ratio:

$$\rho = \left(\frac{P_i}{P_0}\right)^{1/2} = \frac{E_i}{E_0} \tag{4.129}$$

where P and E are the power and electric fields in the oscillators, and the subscripts i and 0 denote the injecting (or master) and receiving (or slave) oscillators. Phase locking occurs when the frequency difference between the two oscillators is sufficiently small:

$$\Delta\omega \leq \frac{\omega_0 \rho}{Q} \tag{4.130}$$

with ω_0 the mean frequency of the two oscillators, which are also taken to have the same value of Q. Equation 4.130 is known as *Adler's relation*. The timescale for locking is given approximately by

$$\tau \sim \frac{Q}{2\rho\omega_0} \tag{4.131}$$

For $\rho \sim 1$, the locking range $\Delta\omega$ is maximized and the timescale for locking is minimized. This facilitates locking of oscillators with larger frequency differences and makes arrays tolerant of oscillator variations. The weak coupling regime, $\rho << 1$, allows a small oscillator to drive a larger one, but takes a corresponding longer time for locking to occur (see Problem 19). Phase locking at high powers has been studied most thoroughly in relativistic magnetrons (see Chapter 7). A second method for phase locking involves prebunching of a beam before it is injected into a microwave source. This has been done in gyroklystrons. A third method is known as *priming* an oscillator. In this case, a locking signal is injected during the start-up phase of the oscillator, which then locks to the injected signal.

4.11 Summary

Many of the fundamental concepts introduced in this chapter will recur throughout the book. The normal modes of rectangular waveguides are denoted TE_{np} and TM_{np} (and, to avoid inconsistency in notational conventions elsewhere, TE_{pn} and TM_{pn} in circular waveguides), where n and p are indices on the field variations in the transverse plane. A normal mode will not propagate through a waveguide below a characteristic frequency, known as the cutoff frequency. The cutoff frequency scales inversely with the cross-sectional dimensions of the guide, so that single-mode propagation is typically confined to relatively narrow guides. High power transmission through a guide demands a large waveguide cross section and a resulting availability of many modes above cutoff. This is known as overmoded operation.

Slow-wave structures support waves with phase velocities less than the speed of light. The cross-sectional structure of these modes can have the characteristics of the TE and TM modes of a smooth-walled waveguide, although as the frequency and wavenumber vary, the cross-sectional structure of a given slow-wave-structure mode can transition from one TE or TM mode to another.

The normal modes of cavities are characterized by an additional index on the axial variations of the fields within, e.g., TE_{npq} (where the ordering of indices is x-y-z for rectangular coordinates and θ-r-z for cylindrical coordinates, by convention). Cavities are characterized by the *quality factor* Q, which measures energy loss per cycle from the oscillating fields in the cavity. Energy loss, and the contributions to Q, comes primarily from two factors: power coupled out as useful microwave radiation and power lost to parasitics. Low Q operation is in many cases desirable in HPM sources.

Resonant interaction at a common frequency and wavenumber between the waveguide or cavity fields and an oscillatory mode in a body of energetic electrons enables the energy transfer from the electrons that generates HPM. Beam bunching is crucial to enforcing the coherence of the waves that are emitted. The classification scheme used here to organize the devices is based on the character of the interactions underlying the generation mechanism in a device.

Functionally, we can also distinguish between devices on an operational basis, denoting them as amplifiers, oscillators, or super-radiant amplifiers. In some cases, certain devices are better suited to operation in one of these different modes, although others can be operated in each of these three under varying conditions. Oscillators tend to operate at a single frequency, depending on their design features; techniques exist, however, to control the phase and, to an extent, the frequency of the output.

Problems

1. For a length of rectangular waveguide in X-band with dimensions a = 2.286 cm and b = 1.016 cm, (a) What is the WR number? (b) What are the cutoff frequencies for the first four propagating modes? Remember that L(cm) = 2.54 × L (inches).
2. Compute the cutoff frequency for the TE_{11} modes in rectangular and circular waveguides with similar dimensions. For the rectangular waveguide, assume a rectangular cross section with a = b = 2 cm. For the circular waveguide, assume a diameter of $2r_0$ = 2 cm. Repeat the exercise for the TM_{11} mode in both.
3. Gyrotrons operate near the cutoff frequency for the cylindrical interaction cavity. To understand the frequency spacings involved, consider the spacing in cutoff frequencies for a cylindrical waveguide with a radius of 2 cm. (a) First compute the cutoff frequencies for the TE_{11} and TE_{12} modes. What is the spacing in hertz, and how much higher is the second mode than the first, on a percentage basis? (b) Next compute the cutoff frequencies for the TE_{82} and TE_{83} modes. Again, what is the spacing in hertz, and how much higher is the second mode than the first, on a percentage basis?
4. For a maximum allowable field at the wall of 100 kV/cm, (a) What power can a rectangular waveguide propagate in fundamental mode at 3 GHz? (b) What power can a circular waveguide propagate in the lowest-frequency TM mode at 3 GHz? Assume that the waveguide is cut off to propagation for modes above the ones designated here; state the dimensions you use.
5. Consider a circular waveguide carrying 5 GW of power in the TM_{01} mode. How large must the radius be to keep the electric field at the wall at 200 kV/cm? At that radius, how many of the TM_{0n} modes are allowed to propagate in the waveguide?

6. Consulting the formulary, what is the skin depth of aluminum at 10 GHz?
7. Estimate the lower and upper frequencies of the lowest passband for an axially varying slow-wave structure with a sinusoidally rippled wall with a mean radius of 4 cm and a ripple period of 1 cm.
8. Estimate the Q of a copper-lined cavity operating at 35 GHz, with a diameter of 3 cm and a length of 5 cm, with the ends partially capped.
9. Diode impedance is the ratio of voltage over current. What diode impedance is required to produce 5 GW of microwaves from a source with an efficiency of 20% when the diode operates at a voltage of 1.5 MV?
10. For efficient energy transfer, assume you want to match the impedance of a diode to an oil-insulated pulse-forming line with an impedance of 43 Ω. If the voltage on the diode is to be 500 keV, and the gap must be at least 2 cm to avoid gap closure during the pulse due to plasma from the cathode, what cathode diameter do you need?
11. Prove that the expression for the cathode current density in a cylindrical diode (Equation 4.106) yields the expression for the current density in a planar diode (Equation 4.104) in the limit of a near-planar diode, where r_a approaches r_c.
12. Consider a coaxial diode emitting radially from an emitting region L = 3 cm long on a cathode at radius r_c = 1.58 cm toward an anode at r_a = 2.1 cm, with an anode–cathode voltage of 400 kV. These are the radii of the A6 magnetron, but we assume there is no axial magnetic field, so that the current can flow across the gap. Compute the current flowing across the gap. Compare the value of the current to the same current for a planar diode with the same gap and the same emitting area as the cathode in the cylindrical diode.
13. At what voltage will a 40-kA beam from a diode with a 4-cm cathode radius and a 2-cm anode–cathode gap form a pinch?
14. A cylindrical electron beam of uniform current density and radius r_b is emitted from a planar diode with a gap of 2 cm and an accelerating voltage of 1.5 MV. It passes through a planar, thin-foil anode into a cylindrical drift tube 4.5 cm in radius. (a) If we assume that the beam enters the drift space with the same radius as the radius of the circular face of the cathode, which has a radius r_c, what is the minimum value of r_c to get virtual cathode formation? (b) What is the radius of the cathode at which the beam current is twice the space-charge-limiting current in the drift tube?
15. If we inject a 5-kA electron beam with a radius of 2 cm from a 1-MV diode into a drift tube 3 cm in radius, what value of axial magnetic field is required to keep its rotational frequency — the frequency for rotation of the beam about its axis in the slow rotational mode — below 500 MHz?
16. The basic relativistic magnetron, termed the A6 because it uses six cavities in its resonant structure (see Chapter 7), has a cathode and anode radii of 1.58 and 2.1 cm, respectively, and operates at 4.6 GHz at a voltage of 800 keV. What magnetic field is required to insulate it?
17. A 3-MeV electron beam passes through a wiggler magnet array in which magnets of opposing polarity are spaced 5 cm apart. What is the wiggler frequency in this system?
18. What is the minimum magnetic field required to operate a gyrotron at 100 kV in a 3-cm-radius cavity?
19. Two high power oscillators both have the same 3-GHz frequency and Q = 100, values typical of HPM sources. Their pulse durations are 100 nsec, also typical of HPM sources. The bandwidth of each is 1%. They are driven in parallel by a pulsed power unit, so they radiate simultaneously. They are to be phase locked together to add their powers before being radiated from an antenna. How well coupled do they have to be, i.e., what injection ratio is required if they are to lock within 1/3 of their pulse lengths? If their rise time is Q cycles of the 3-GHz frequency and they are to lock within the rise time, what injection ratio is required?

References

1. Neuber, A.A., Laurent, L., Lau, Y.Y., and Krompholz, H., Windows and RF breakdown, in *High-Power Microwave Sources and Technology*, Barker, R.J. and Schamiloglu, E., Eds., IEEE Press, New York, 2001, p. 346.
2. Kurilko, V.I. et al., Stability of a relativistic electron beam in a periodic cylindrical waveguide, *Sov. Phys. Tech. Phys.*, 24, 1451, 1979 (*Zh. Tekh. Fiz.*, 49, 2569, 1979).
3. Bromborsky, A. and Ruth, B., Calculation of TM_{on} dispersion relations in a corrugated cylindrical waveguide, *IEEE Trans. Microwave Theory Tech.*, MTT-32, 600, 1984.
4. Swegle, J.A., Poukey, J.W., and Leifeste, G.T., Backward wave oscillators with rippled wall resonators: analytic theory and numerical simulation, *Phys. Fluids*, 28, 2882, 1985.
5. Guschina, I.Ya. and Pikunov, V.M., Numerical method of analyzing electromagnetic fields of periodic waveguides, *Sov. J. Commun. Tech. Electron.*, 37, 50, 1992 (*Radiotekh. Elektron.*, 8, 1422, 1992).
6. Leifeste, G.T. et al., Ku-band radiation produced by a relativistic backward wave oscillator, *J. Appl. Phys.*, 59, 1366, 1986.
7. Petit, R. and Cadilhac, M., Sur la diffraction d'une onde plane par un reseau infiniment conducteur, *C. R. Acad. Sci. Paris Ser. B*, 262, 468, 1966.
8. Millar, R.F., On the Rayleigh assumption in scattering by a periodic surface: II, *Proc. Camb. Phil. Soc.*, 69, 217, 1971.

9. Watanabe, T. et al., Range of validity of the Rayleigh hypothesis, *Phys. Rev. E*, 69, 056606-1, 2004.
10. Kroll, N., The unstrapped resonant system, in *Microwave Magnetrons*, Collins, G.B., Ed., McGraw-Hill, New York, 1948, pp. 49–82.
11. Child, C.D., *Phys. Rev.*, 32, 492, 1911; Langmuir, I., The effect of space charge and residual gases on thermionic currents in high vacuum, *Phys. Rev.*, 2, 450, 1913.
12. Langmuir, I. and Blodgett, K.B., Current limited by space charge between coaxial cylinders, *Phys. Rev.*, 22, 347, 1923.
13. Jory, H.R. and Trivelpiece, A.W., Exact relativistic solution for the one-dimensional diode, *J. Appl. Phys.*, 40, 3924, 1969.
14. Friedlander, F., Hechtel, R., Jory, H.R., and Mosher, C., Varian Associates Report DASA-2173, 1965.
15. See, for example, Davidson, R.C., *Theory of Nonneutral Plasmas*, W.A. Benjamin, Reading, MA, 1974.
16. Krall, N.A. and Trivelpiece, A.W., *Principles of Plasma Physics*, McGraw-Hill, New York, 1971, pp. 138–143.
17. Kadomtsev, B.B., Mikhailovskii, A.B., and Timofeev, A.V., Negative energy waves in dispersive media, *Sov. Phys. JETP*, 20, 1517, 1965 (*Zh. Eksp. Tekh. Fiz.*, 47, 2266, 1964).
18. Kuzelev, M.V. and Rukhadze, A.A., Stimulated radiation from high-current relativistic electron beams, *Sov. Phys. Usp.*, 30, 507, 1987 (*Usp. Fiz. Nauk*, 152, 285, 1987).
19. Friedman, M. et al., Relativistic klystron amplifier, *Proc. SPIE*, 873, 92, 1988.
20. Brejzman, B.N. and Ryutov, D.D., Power relativistic electron beams in a plasma and a vacuum (theory), *Nucl. Fusion*, 14, 873, 1974.
21. Walsh, J., Stimulated Cerenkov radiation, in *Novel Sources of Coherent Radiation*, Jacobs, S., Sargent, M., and Scully, M., Eds., Addison-Wesley, Reading, MA, 1978, p. 357.
22. Bratman, V.L. et al., Stimulated scattering of waves on high-current relativistic electron beams: simulation of two-stage free-electron lasers, *Int. J. Electron.*, 59, 247, 1985.
23. Elias, L.R., High-power, CW, efficient, tunable (UV through IR) free electron laser using low-energy electron beams, *Phys. Rev. Lett.*, 42, 977, 1979.
24. Carmel, Y., Granatstein, V.L., and Gover, A., Demonstration of a two-stage backward-wave-oscillation free-electron laser, *Phys. Rev. Lett.*, 51, 566, 1983.

5

Enabling Technologies

5.1 Introduction

The rapid development of high power microwaves (HPM) during the 1980s was due to the availability of a technology base that had been developed for other applications. Figure 5.1 shows the subsystems of an HPM device operating in an HPM facility. Pulsed electrical systems, referred to as *pulsed power*, were developed in the 1960s to enable nuclear weapons effects simulation. Later, inertial confinement fusion became a driver for pulsed power technology. HPM has largely made use of existing pulsed power equipment to perform initial experiments. The intense beams generated by pulsed power devices have been studied in some detail, including beam generation and beam propagation in various media such as vacuum, plasma, and gases. In diagnostics for HPM, the bulk of the devices used are conventional diagnostic techniques with additional attenuation to reduce power levels before the diagnostic data are taken. An exception to this is calorimetry, which must handle high electric fields but little total energy. Some microwave components, such as waveguides, have been borrowed from the conventional microwave technology base. For example, evacuated waveguides of conventional design can support electric fields of 100 kV/cm for short pulses. Similarly, antennas have used direct extrapolation of conventional antenna design with some care taken to avoid air breakdown, with the major exception of the Impulse Radiating Antenna (IRA; see Sections 5.5 and 6.3). With the emergence of facilities specifically designed to study HPM effects and develop HPM technologies, the primary issues are the operational and safety constraints for protection of personnel and ancillary electronic equipment from the effects of high power pulses.

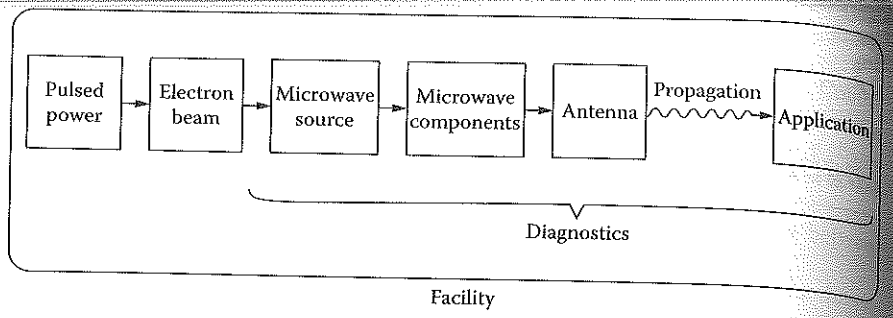

FIGURE 5.1
Flow diagram of HPM system in a facility.

5.2 Pulsed Power

The short, intense pulses of electricity needed to drive HPM loads are obtained by a process of pulse compression. The energy taken from a low-voltage, long-pulse system is compressed in time, increasing both voltage and current at the expense of pulse duration.[1] Electrical requirements of HPM sources encompass a wide range of voltages, currents, and pulse durations.[2] Most initial HPM source physics questions can be adequately addressed in short-pulse experiments (~100 nsec), which are also preferred because they are easy to carry out, relatively inexpensive, and relatively small. There are also difficulties, such as breakdown, in operating high power sources for longer durations. Consequently, the key distinguishing parameters of most devices are the voltage, current, and their ratio, *impedance*. The subset of electrical voltage–impedance parameter space into which HPM source technologies fall is shown in Figure 5.2. With voltages of <100 kV and impedances of >1000 Ω, conventional microwave applications (radar, electronic countermeasures, communications) lie at the low power end (power = V^2/Z). Most, but not all, present-day HPM sources cluster around 10 to 100. Voltages generally span the range of 0.1 to 1 MV, but some sources have been operated up to 4 MV.

The immediate implication of Figure 5.2 is that efficient transfer of electrical energy will require pulsed power technologies that span a substantial impedance range. When circuit elements do not have the same impedance, voltage, current, and energy transferred to the downstream element can be very different (Figure 5.3). The voltage gain V_2/V_1 and energy transfer ratio E_2/E_1 for a transmission line transferring power to a longer output line (so that reflections from the output line can be neglected during the main pulse) are

$$\frac{V_2}{V_1} = \frac{Z_2}{Z_1 + Z_2} \tag{5.1}$$

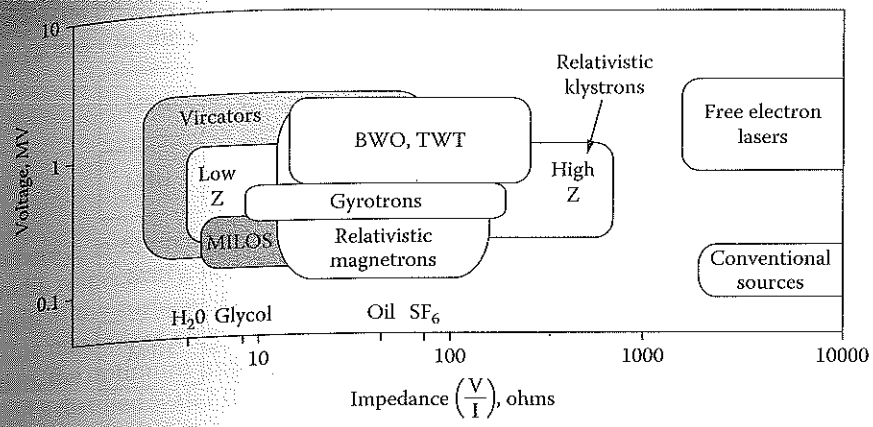

FIGURE 5.2
Voltage and impedance parameter space for HPM and pulsed conventional sources. Optimum impedances for widely used pulse line insulators (water, glycol, oil, SF_6) are shown.

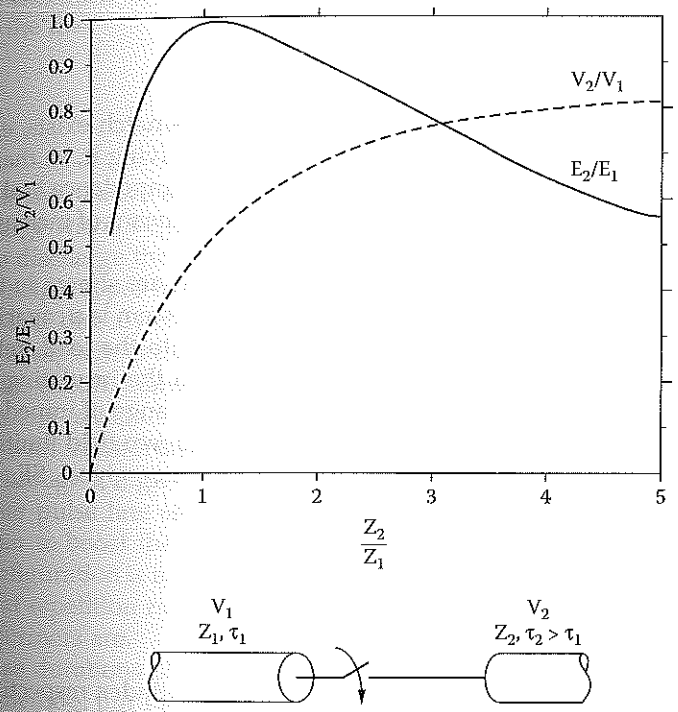

FIGURE 5.3
Energy transfer and voltage ratios between transmission line (1) and load (2) as a function of impedance ratio.

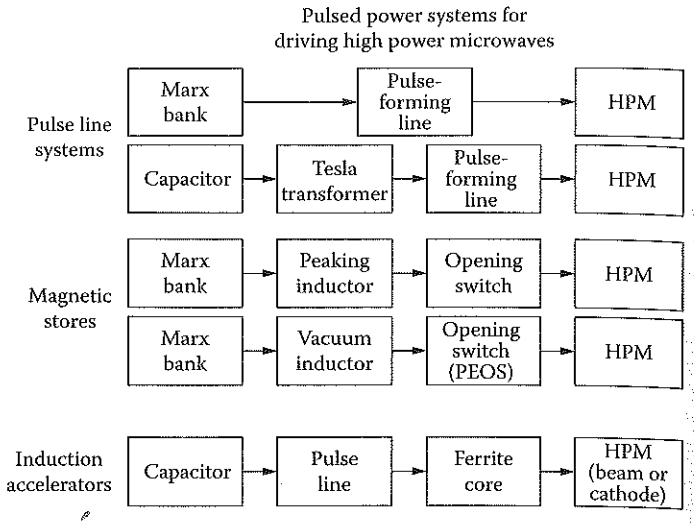

FIGURE 5.4
Types of pulsed power systems for driving HPM loads.

$$\frac{E_2}{E_1} = \frac{4Z_1Z_2}{[Z_1 + Z_2]^2} \tag{5.2}$$

Efficient energy transfer suffers if impedance mismatch exists, especially if the load is of lower impedance than the circuit driving it, so that it looks like a short. Mismatching upward to a higher load impedance looks like an open circuit, but is sometimes used as an inefficient means of increasing load voltage (see Problem 1).

The types of pulsed power systems used in HPM are shown in the block diagrams of Figure 5.4. The most commonly used system is a capacitor bank driving a *pulse-forming line* that, when switched into the load, releases its energy in two transit times at the speed of light in the insulating medium of the line. Coaxial transmission lines span a large range of impedance and voltage depending upon their characteristic breakdown field limits and the insulating dielectric between the electrodes (oil, water, glycol, SF_6, air). The impedance depends upon the dielectric constant, ε:

$$Z = \frac{1}{2\pi}\sqrt{\frac{\mu}{\varepsilon}}\ln b/a \tag{5.3}$$

where b and a are the outer and inner radii of the cylinder, respectively. The energy density,

$$E = 1/2\ \varepsilon E^2 \tag{5.4}$$

depends linearly upon the dielectric constant, ε. Here E is the electric field at radius r in the dielectric and V the applied voltage:

$$E = \frac{V}{r\varepsilon_r \ln\frac{b}{a}} \tag{5.5}$$

where ε_r is the relative dielectric constant and b and a the outer and inner radii, respectively. For fixed outer diameter and applied voltage, the electric field at the surface of the inner cylinder is a minimum when b/a = e = 2.71. This maximizes energy density while avoiding breakdown. For this condition, the optimum impedance of an oil line is 42; an ethylene glycol line, 9.7; and a distilled water line, 6.7. Optimum coaxial impedances are shown along the horizontal axis of Figure 5.2. On the other hand, liquid energy density is largest for water (0.9 relative to mylar), intermediate for glycol (0.45), and lowest for oil (0.06). The solid dielectric mylar has the highest energy density, but if broken, it will not recover.

Low-impedance microwave loads will therefore be a better match to water-lines, and high-impedance loads will better match oil lines. The duration of the pulse that can be extracted from a line is determined by the electrical length of the line,

$$\tau = \frac{2\varepsilon_r L}{c} \tag{5.6}$$

where ε_r is the relative dielectric constant and L is the line length. Note that the discharge wave, begun by closing a switch at one end, must make two transits to discharge the line.

Two principal types of pulse-forming line systems are used in HPM. The first is a Marx directly charging a PFL (Figure 5.5). The *Marx generator* is an assembly of capacitors that are charged in parallel and then quickly switched into a series circuit, allowing the original charging voltage to be multiplied by the number of capacitive stages in the Marx. Marx generators are usually insulated with transformer oil to reduce their size. The PFL is switched into the load through a high-voltage closing switch.

The other pulse line scheme uses a capacitor bank at low voltage and a transformer to boost the voltage and charge the pulse line. The advantage of this configuration is in repetitive operation. Marx generators are generally not used at repetition rates above 10 Hz because of losses and fault modes, but transformers are.

For pulse durations of <200 nsec, the PFL is the appropriate pulse compression method, but PFLs become very large for longer pulse lengths. For such lengths, discrete inductive and capacitive components are used to assemble a *pulse-forming network* (PFN), which is designed to generate a Fourier series approximating the desired waveform. An example of a PFN

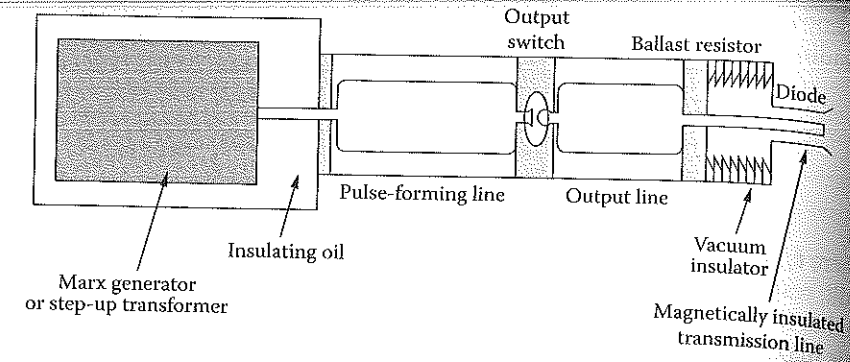

FIGURE 5.5
Schematic of a pulse-forming line system. Many elements are common to other approaches in Figure 5.4.

is shown in Figure 5.6a, and the output pulse from this circuit is shown in Figure 5.6b. In general, PFNs produce a pulse with voltage oscillations, typically an overshoot at the beginning of the pulse and an undershoot at the end. Voltage variations always affect the performance of the source, and one of the key features of matching pulsed power to HPM sources is sensitivity of the load performance to the applied voltage. The concern is usually for voltage flatness during the bulk of the pulse. PFN circuits can be optimized for voltage flatness.

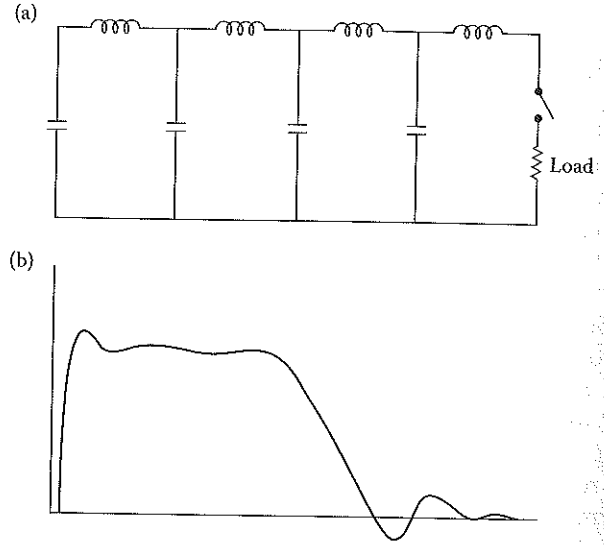

FIGURE 5.6
Pulse-forming networks: (a) typical distributed LC (inductor-capacitor) circuit; (b) output pulse has fast rise, overshoot, and slow fall time with undershoot. Durations are typically from 0.5 to 10 μsec.

Switching of PFLs and PFNs into the load is usually done by a spark gap switch using gas as a dielectric insulating medium. Because most microwave sources require precision in the applied voltage, and spark gaps have substantial variation in pulse-to-pulse voltage output, spark gaps in HPM systems are usually externally triggered. For repetitive operation the insulating gas is circulated to achieve faster recovery, carry away debris evolved from the electrodes, and remove heat dissipated in the gap. The typical timescale for recovery of dielectric strength in an uncirculated gas is ~10 msec; arc switches operating at >1 kHz with gas flow have been reported.[3]

When HPM sources are brought into development, they typically initially operate at powers lower than intended. Therefore, they will draw less current and operate at higher impedance than the experiment has been designed for. A common technique providing a match to a microwave load whose impedance will drop as it is developed is to use a ballast resistor (Figure 5.5), a liquid resistor with adjustable resistance so that the parallel combination with the microwave load provides a match to the pulsed power system.

When the electrical pulse exits the pulse-forming regions (filled with liquid or gas) and enters the vacuum region of the microwave source, it passes through a solid dielectric interface. The typical interface is composed of a stack of insulator rings separated by metal grading rings. The surface of the insulator rings is inclined 45° to the grading rings. The flashover strength of such construction is three to four times that of a straight cylinder. Detailed design is necessary in order to distribute the potential uniformity across the stack, giving roughly equal voltage across each element of the insulator. The typical electric field is 100 kV/cm.

In the vacuum region, insulation is provided by the magnetic field of the pulsed current itself. The typical magnetically insulated transmission line[4] is designed with an impedance about three times that of the load, so that sufficient magnetic field is produced to confine any electrons emitted from the feed.

5.2.1 Magnetic Stores

The second type of pulsed power system for HPM is the *magnetic store* device (Figure 5.4). Interest in magnetic storage is due to the possibility of producing compact accelerators, since the energy density of magnetic storage is one to two orders of magnitude higher than of electrostatic storage systems. Typically, a Marx bank charges a vacuum inductor to peak current, then the key component — the *opening switch* — opens and a large transient voltage appears across the load due to the back-EMF (Electro-Motive Force) of the collapsing magnetic flux in the inductor. Because the peak voltage appears only at the load, and voltage sets the size of components, the storage device can be made compact without danger of internal arcing and shorting. Despite these potential advantages, magnetic storage is not commonly employed for three reasons. First, the L dI/dt voltage across the load has a triangular